EPM–RT–2005-07

OPTIMAL CONTROL OF INDUCTION HEATING FOR SEMI-SOLID METAL FORMING

Hui Jiang, The Hung Nguyen, Michel Prud'homme
Département de Génie mécanique
École Polytechnique de Montréal

Décembre 2005

Poly

ÉCOLE POLYTECHNIQUE MONTRÉAL

EPM-RT-2005-07

OPTIMAL CONTROL OF INDUCTION HEATING FOR SEMI-SOLID METAL FORMING

Hui Jiang
The Hung Nguyen
Michel Prud'homme

Département de Génie Mécanique
École Polytechnique de Montréal

Décembre 2005

Dépôt légal :
Bibliothèque nationale du Québec, 2005
Bibliothèque nationale du Canada, 2005

EPM-RT-2005-07
OPTIMAL CONTROL OF INDUCTION HEATING FOR SEMI-SOLID METAL FORMING
par : Hui Jiang, The Hung Nguyen, Michel Prud'homme
Département de génie mécanique
École Polytechnique de Montréal

Abstract

Thixoforming technique requires heating the feedstock to a semi-solid state with a uniform temperature distribution, a uniform globular microstructure and an optimum liquid fraction. The skin effect of induction heating results in an exponential heat source (power density) profile within the semi-solid material. In this study, the conjugate gradient method in conjunction with the adjoint method is used to find a heating process to achieve a uniform temperature distribution along the radius of a cylinder in a relatively short time. It is found that a modified CGM may provide a satisfactory heating strategy. The physical and mathematical models take into account the temperature-dependent thermo-physical properties. Radiative and convective heat losses and different heating frequencies are also considered.

Introduction

Semi-solid metal (SSM) *forming*, originally introduced by Merton C. Flemings at MIT in 1970's, has become a competitive technique to produce parts for the automotive industry. Comparing to conventional methods such as gravity die-casting and squeeze casting which have various problems such as blowholes, segregation, and thermal defects of the die, SSF requires heating the work piece to the semi-solid state with coexisting liquid and solid phases. It may increase flow viscosity and decrease the processing temperature during casting process, leading to a laminar flow and lower solidification shrinkage and therefore a higher quality of cast products by prevention of entrapment of gas. Its advantages also include excellent surface quality, tight tolerances, high strength, low level of porosity, fine microstructure, energy saving, etc [1-5].

Thixoforming technique usually requires reheating pre-processed feedstock with a fine and non-dendritic structure to a liquid fraction of about 40%~50%. At such a liquid fraction, the rheological properties of the semi-solid alloys are very sensitive to variations in the liquid portion. So the heating process must be accurately controlled to achieve a uniform temperature distribution in the material and necessary liquid fraction. On the other hand, the heating process is required to be relatively rapid to maintain the initial globular microstructure. Otherwise, the semi-solid alloys will not display thixotropic behaviors under shear and thus would not fill the die cavity properly [6-7].

The traditional heating technique in metallurgy industries is related to the gas-fired furnaces because of its low cost. However, gas-fired furnaces require a very long heating tunnel to create the temperature uniformity, and this technique results in poor surface quality due to scale, decarburization, oxidation, coarse grains etc. Nowadays *induction heating* is the most commonly used method in commercial production applications especially in semi-solid metal processing because that is a non-contact, clean, compact and fast method and the input power can be easily controlled. However, induction heating has its inherent drawback of non-uniformity of heating due to the so-called *skin effect*, *end effect* and *electromagnetic transverse edge effect*. In this paper, only skin

effect is considered and the other two effects might be ignored. Because of the skin effect, most power density (heat source) is concentrated on the surface, and decays exponentially below the surface. Then the outside will heat more quickly than the inside; 80%~86% of the heat is produced in the surface layer which is called *current penetration depth*. The non-uniform temperature distribution along the radius of the material is called *surface-to-core temperature profile* [2, 8, 9, 10]. The skin depth is a function of frequency and material properties, it decreases when frequency increases. Considering the maximum electrical efficiency and minimum electromagnetic forces, the commercial machines often work at a frequency of more than 10kHz. Such a high frequency also makes the system more compact.

In order to achieve a uniform temperature by using induction heating, three kinds of heating methods have been frequently applied into the SSF: (1) Fixed coil method: a billet is heated in the same coil; input power varies according to the temperature values measured by the sensors embedded within the material; (2) Multi-coils method: a billet passes through a series of coils sequentially and reaches to semi-solid state in the last coil. A rotation disk induction heater obtained the patent of semi-solid metal heating (American Patent 4,569,218) in 1986; (3) Hybrid method: The researchers at Materials Research Laboratory of Taiwan combined these two methods and modified the electrical and temperature control circuit. These methods essentially are similar: if the temperature reaches at some values, cut or decrease the input power. The heating procedure is determined by experiments and/or automatic control method. However, the shortage is also obvious: the strategy may not be the "best", the heating time may be long, and if the size of material or material itself or the operating frequency of induction heater changed, the experiments must be repeated.

The heating control problem is essentially an inverse problem of determining the time-dependent heat source (power density) to obtain the targeted temperature distribution. In 1960, this kind of optimal control problem in distributed-parameter system was firstly proposed by Butkovskii and Lerner

[11]. Sakawa [12, 13] used a variational method, Cavin and Tandon [14] applied a finite element method, Meric [15, 16] adopted conjugate gradient method to solve the linear and nonlinear boundary control problems in the 60s and 70s of last century. In the last two decades, the solution algorithms were further improved due to the fast development of optimization and inverse problem techniques. Kelley and Sachs [17] introduced a Steihaug trust-region-conjugate-gradient method with a smoothing step at each iteration to solve a 1-D boundary heat flux control problem. Huang [18] solved a similar boundary control problem with temperature-dependent thermal properties by regular conjugate gradient method. The same control problem was extended to 3-D geometries by Huang and Li [19]. Chen and Ozisik [20, 21] estimated the optimum strength of heat sources by a similar algorithm used in [15, 16].

These optimization techniques have not been applied to the semi-solid forming. The objective of this study is to determine an optimal heating strategy to achieve a uniform temperature distribution along the radius of a cylindrical billet within a relatively short time. In this study, all thermal properties are considered temperature-dependent, the heat source is a function of time and space, and surface heat radiation and convection are included.

Problem Definition

A metal slug with a diameter of 76mm and a height of 152mm is vertically placed into an induction coil unit (FIG.1). The power supply generates an alternating current at 10KHz. In order to obtain a uniform liquid fraction and a good consistent viscosity, the billet temperature should be kept within the range of 575-585℃ through the entire cross-section before the material flow into the die cavity under a pressure. In this report, only the one-phase model is considered, i.e., the targeted temperature is set below the value at which the alloy starts to melt. The two-phase model is the subject of on-going research. Due to the "skin" effect, the temperature is not uniform along the radius of the billet, as $T_{surface}$ must be higher than T_{center}. In addition, the slug surface is convectively cooled in order to avoid the 'elephant foot' effect, and to decrease

the temperature difference between the center and surface. The electromagnetic transverse edge effects are not to be considered because of the cylindrical geometry of the work-piece, if the 'elephant foot' effect could be controlled. If the induction heater is well designed and there is no coil overhang, then the end effecs and the top-to-bottom thermal gradients can be ignored. The physical model can be therefore simplified to one-dimensional case. In this paper, the problem is solved in a Cartesian coordinates system.

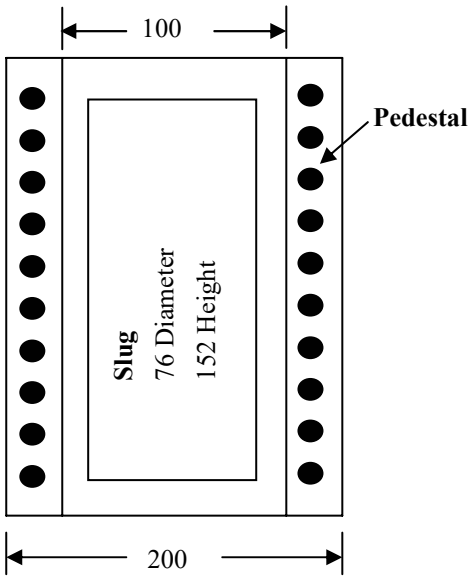

FIG. 1 Schematic of Induction Heating Coil and Slug

Mathematical Model

Suppose a metal bar is cooled from the right side by convection and radiation, and its left side is adiabatic. The initial temperature field and boundary conditions are assumed to be known. A heat source which is a function of space and time is generated by induction heating. The heat conduction problem is governed by following non-linear equation:

$$\rho(T)c_p(T)\frac{\partial T}{\partial t}=\frac{\partial}{\partial x}\left(k(T)\frac{\partial T}{\partial x}\right)+S(x,t) \qquad (1)$$

where $S(x,t)$ denotes inner heat source; ρ is the density; c_p is the specific heat and k is the thermal conductivity. Suppose that the heat source may be expressed as $S(x,t)=G(t)\cdot H(x)$ and let us define volumetric heat capacity $C(T)=\rho(T)c_p(T)$, Eq.(1) may be rewritten as

$$C(T)\frac{\partial T}{\partial t}=\frac{\partial}{\partial x}\left(k(T)\frac{\partial T}{\partial x}\right)+G(t)\cdot H(x) \tag{2}$$

The corresponding boundary and initial conditions are as

$$k\frac{\partial T}{\partial x}\bigg|_{x=0}=0,\ k\frac{\partial T}{\partial x}\bigg|_{x=L}=p(T)+q(t),\ T(x,0)=f(x) \tag{3}$$

where $p(T)=\dfrac{\sigma_b\left(T_s^4-T_p^4\right)}{\dfrac{1}{\varepsilon_s}+\dfrac{1-\varepsilon_p}{\varepsilon_p}\dfrac{As}{A_p}}$ is the radiative heat flux, $q(t)$ is the convective heat flux and Stefan-Boltzmann constant $\sigma_b=5.67\times10^{-8}\,W/m^2\cdot K^4$. The subscript 's' denotes the surface of slug, 'p' denotes inner surface of pedestal. Suppose that the pedestal is cooled by cooling water, and $T_p\equiv T_{ambient}$.

Heat source distribution

From Maxwell equations, it can be proved that the induced current density decreases exponentially from the periphery towards to the center [22]. The distribution of current density within a cylinder-shaped material is of the form:

$$I(x)=I_0\cdot e^{-(L-x)/\delta}$$

Here I_0 is the maximum eddy current on the surface, L is radius of material. From Joule's law, we may get the distribution of power density (heat source) along the direction of radius:

$$S(x)=S_0\cdot\frac{I^2}{I_0^2}=S_0\cdot e^{-2(L-x)/\delta} \tag{4}$$

Here S_0 denotes the maximum power density (heat source) on the surface, δ is penetration (skin) depth. Then the time-dependent heat source may be expressed as:

$$S(x,t)=G(t)\cdot e^{-2(L-x)/\delta} \tag{5}$$

For metal materials, the *skin depth* can be expressed by resistivity, permeability of the material and the current frequency:

$$\delta=503.3\sqrt{\frac{R}{\mu_r f}} \tag{6}$$

where R: is the load resistivity (in ohms-meters); μ_r is the load relative magnetic permeability; f is the current frequency (in Hz). For aluminum (alloys) and copper, $\mu_r \cong 1$. R is proportional to the temperature. For Aluminum alloy A356, $R \approx 3.89\times10^{-8} + 1.53\times10^{-10} T\ (\Omega\cdot m)$. The power density (heat source) distribution of A356 along the non-dimensional radius is shown in FIG.2. It is found that the temperature of A356 does not influence the heat source distribution too much within a range from 20℃ to 570℃. The resistivity may be therefore as independent of temperature. However, the current frequency considerably affects the heat source distribution. Generally speaking, as the frequency is smaller, the temperature distribution becomes more uniform.

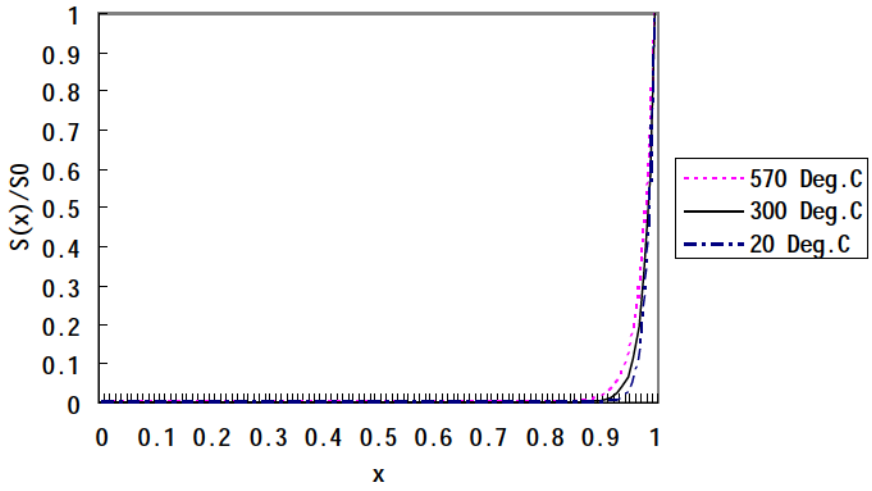

FIG.2.1: Heat Source Distribution of A356, f=10000Hz

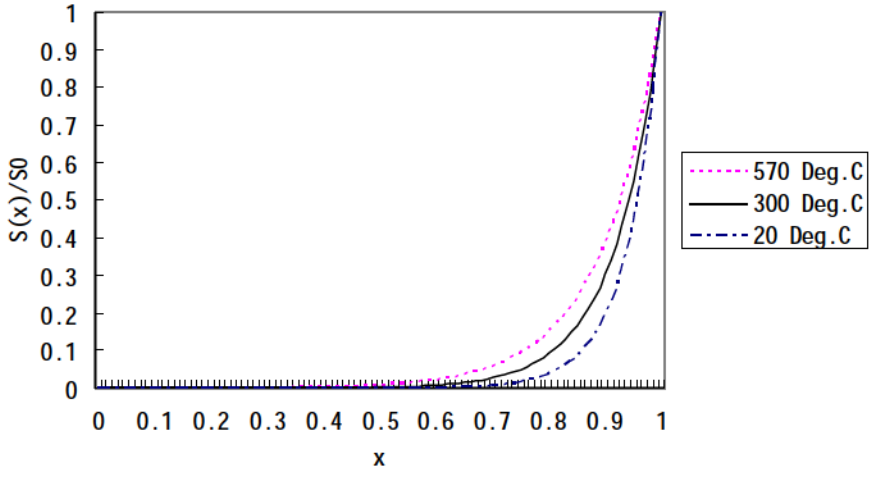

FIG.2.2: Heat Source Distribution of A356, f=500Hz

Optimum Heating Control Problem

According to the discussion above, the heat source distribution $H(x)$ will be fixed by the operating frequency of the induction heater. If the surface cooling flux $q(t)$ is given, our objective is to determine the timewise strength of heat source $G(t)$ such that the final temperature $T(x,t_f)$ is equal to the targeted value $T_E(x)$. The solution is obtained by minimizing the error functional E which is defined as:

$$E(G)=\frac{1}{2}\int_0^L \left[T(x,t_f)-T_E(x)\right]^2 dx+\frac{\xi}{2}\int_0^{t_f} G^2(t)dt \tag{7}$$

where ξ is the regularization parameter. Among various optimization techniques, conjugate gradient method is frequently adopted because of its efficiency and self-regularization character. As an iterative algorithm, the search direction and step size must be determined. The search direction is related to the gradient of E which is obtained by solving an adjoint problem, while the optimal step size may be determined by solving a sensitivity problem.

Sensitivity Equation

The sensitivity temperature $\tilde{T}$ is defined as the directional derivative of T at G in the direction ΔG:

$$\tilde{T}=\lim_{\varepsilon\to 0}\frac{T(G+\varepsilon\Delta G)-T(G)}{\varepsilon} \tag{8}$$

Starting from Eq. (2), the sensitivity equation may be easily obtained:

$$\frac{\partial(C\tilde{T})}{\partial t}=\frac{\partial^2(k\tilde{T})}{\partial x^2}+\Delta G\cdot H \tag{9}$$

Similarly we may get the initial and boundary conditions:

$$\tilde{T}(x,0)=0,\ \left.\frac{\partial(k\tilde{T})}{\partial x}\right|_{x=0}=0,\ \left.\frac{\partial(k\tilde{T})}{\partial x}\right|_{x=L}=\left.(p'\cdot\tilde{T})\right|_{x=L} \tag{10}$$

Adjoint Equation

According to the definitions of the error function and sensitivity, it is not difficult to derive the following equation:

$$D_{\Delta G}E(G)=\int_0^L\left\{\tilde{T}(x,t_f)\cdot\left[T(x,t_f)-T_E\right]\right\}dx+\xi\int_0^{t_f}(G\cdot\Delta G)dt=\int_0^{t_f}(\nabla E\cdot\Delta G)dt \tag{11}$$

If the adjoint temperature $\overline{T}$ and Eq. (9) are respectively treated as Lagrange multiplier and constraint, we may rewrite Eq. (11) as

$$\begin{aligned}D_{\Delta G}E(G)=&\int_0^L\left\{\left[T(x,t_f)-T_E\right]\cdot\tilde{T}(x,t_f)\right\}dx+\xi\int_0^{t_f}(G\cdot\Delta G)dt\\&+\int_0^{t_f}\int_0^L\overline{T}\left[\frac{\partial(C\tilde{T})}{\partial t}-\frac{\partial^2(k\tilde{T})}{\partial x^2}-\Delta G\cdot H\right]dxdt\end{aligned} \tag{12}$$

Considering the initial and boundary conditions of the sensitivity problem,, we derive the following adjoint equation after some algebra:

$$C\frac{\partial\overline{T}}{\partial t}+k\frac{\partial^2\overline{T}}{\partial x^2}=0\ \text{ or }\ C\frac{\partial\overline{T}}{\partial\tau}=k\frac{\partial^2\overline{T}}{\partial x^2},\ \tau=t_f-t \tag{18}$$

$$k\frac{\partial\overline{T}}{\partial x}\bigg|_{x=0}=0,\ k\frac{\partial\overline{T}}{\partial x}\bigg|_{x=L}=(p'\cdot\overline{T})\big|_{x=L},\ \overline{T}(x,t_f)=-\frac{T(x,t_f)-T_E(x)}{C} \tag{19}$$

Eq.(12) then becomes

$$D_{\Delta G}E(G)=\int_0^{t_f}\left(\xi\cdot G-\int_0^L\overline{T}Hdx\right)\Delta Gdt \tag{20}$$

Comparing Eq.(20) and (11), it follows that the gradient of the error functional is

$$\nabla E=\xi\cdot G-\int_0^L\overline{T}(x,t)H(x)dx \tag{21}$$

Regular Conjugate Gradient Method

The iterative formula and the conjugate search direction may be expressed as:

$$G^{k+1}=G^k+\alpha^kP^k \tag{22}$$

$$P^k=-\nabla E^k+\beta^kP^{k-1} \tag{23}$$

The optimum step size may be derived from the value that makes the first order derivative of E in the direction α^k vanish:

$$\alpha^k = -\frac{\int_0^1 \left(T^k - T_E\right)\tilde{T}^k dx + \xi \int_0^{t_f} G^k P^k dt}{\int_0^1 (\tilde{T}^k)^2 dx + \xi \int_0^{t_f} (P^k)^2 dt} \tag{24}$$

The overall CGM (Polak-Ribiere version) algorithm may be summarized as follows:

1. Set an initial initial guess $G^0 = G_0(t)$, set the iteration counter k = 0.

2. Solve the direct problem with G^k to obtain T^k.

3. Evaluate the difference $T^k(x, t_f) - T_E$.

4. Solve the adjoint problem backward in time for $\bar{T}^k$.

5. Evaluate the gradient following Eq.(21).

6. Calculate the search direction P^k:

$$P^k = \begin{cases} -\nabla E^k & \text{if} \quad k = 0 \\ -\nabla E^k + \beta^k P^{k-1} & \text{if} \quad k > 0 \end{cases} \tag{25}$$

$$\beta^k = \frac{\int_0^{t_f} (\nabla E^k - \nabla E^{k-1}) \nabla E^k dt}{\int_0^{t_f} (\nabla E^{k-1})^2 dt} \tag{26}$$

7. Solve the sensitivity problem with $\Delta G = P^k$ to obtain $\tilde{T}^k$.

8. Calculate the step size α^k with Eq. (24).

9. Update to $G^{k+1} = G^k + \alpha^k P^k$.

10. Set k = k + 1, go back to step 2, repeat until convergence criterion $E^k < \varepsilon$ is satisfied.

Modified Conjugate Gradient Method

The works presented in [17, 19, 23] show that the optimal solutions by regular CGM may tend to a (time-averaged) constant and change steeply near the final time. Such a heating/cooling curve is difficult to be executed in engineering applications. In fact, a modification of the conjugate direction is found to be a good way to improve the profile of optimization solutions [24].

This modified CG method [25-28] is based on the assumption that G(t) is a continuously differentiable function defined as

$$G(t)=\int_0^t \frac{dG(t')}{dt'}dt',\ \Delta G(t)=\int_0^t \frac{d\Delta G(t')}{dt'}dt' \tag{27}$$

which requires

$$G(t=0)=\Delta G(t=0)=0 \tag{28}$$

Applying the rule of differentiation under the integral sign, we have the identity

$$\frac{d}{dt}\int_{t_f}^{t}\int_0^L \overline{T}(x,t')H(x)dxdt'=\int_0^L \overline{T}(x,t)H(x)dx \tag{29}$$

Introducing Eq.(29) into Eq.(11), we obtain

$$D_{\Delta G}E\left(\frac{dG}{dt}\right)\equiv D_{\Delta G}E(G)=\int_0^{t_f}\left\{\left[\frac{d}{dt}\int_{t_f}^{t}\int_0^L \overline{T}(x,t')H(x)dxdt'\right]\cdot\Delta G\right\}dt \tag{30}$$

Integrating the first term of the right hand side of Eq. (30) by parts and rewriting the second term, we get

$$D_{\Delta G}E\left(\frac{dG}{dt}\right)=\left\{\left[\int_t^{t_f}\int_0^L \overline{T}(x,t')H(x)dxdt'\right]\cdot\Delta G\right\}\Bigg|_0^{t_f}-\int_0^{t_f}\frac{d\Delta G}{dt}\left[\int_t^{t_f}\int_0^L \overline{T}(x,t')H(x)dxdt'\right]dt \tag{31}$$

Then

$$D_{\Delta G}E\left(\frac{dG}{dt}\right)=\int_0^{t_f}\frac{d\Delta G}{dt}\left[-\int_t^{t_f}\int_0^L \overline{T}(x,t')H(x)dxdt'\right]dt \tag{32}$$

By comparing Eq.(32) with Eq.(21), we have

$$\nabla E\left(\frac{dG}{dt}\right)=-\int_t^{t_f}\int_0^L \overline{T}(x,t')H(x)dxdt'=\int_t^{t_f}\nabla E dt' \tag{33}$$

The modified search direction is related to the derivative of the direction of descent R^k by the relation

$$p^k=\int_0^t R^k dt' \tag{34}$$

$$R^k=-\nabla E\left(\frac{dG}{dt}\right)+\gamma^k R^{k-1} \tag{35}$$

The conjugate coefficient γ^k is given by Eq. (26) and the gradient of the error function is replaced by $\nabla E\left(\frac{d\Delta G}{dt}\right)$:

$$\gamma^k = \frac{\int_0^{t_f}\left[\nabla E^k\left(\frac{dG}{dt}\right) - \nabla E^{k-1}\left(\frac{dG}{dt}\right)\right]\cdot \nabla E^k\left(\frac{dG}{dt}\right)\cdot dt}{\int_0^{t_f}\left[\nabla E^{k-1}\left(\frac{dG}{dt}\right)\right]^2 \cdot dt} \tag{36}$$

Optimum cooling Control Problem

Suppose that the heat source $S(x,t)$ is known, let us determine the cooling flux $q(t)$ to achieve an as uniform as possible final temperature $T(x,t_f)$. The optimization solution is obtained by minimizing the error functional E which is defined as:

$$E(q) = \frac{1}{2}\int_0^L \left[T(x,t_f) - T_E(x)\right]^2 dx + \frac{\xi}{2}\int_0^{t_f} q^2(t)dt \tag{37}$$

And we follow the similar procedure to determine the search direction and the step size.

Sensitivity Equation

The sensitivity temperature $\tilde{T}$ is defined as the directional derivative of T at q in the direction Δq:

$$\tilde{T} = \lim_{\varepsilon\to 0}\frac{T(q+\varepsilon\Delta q) - T(q)}{\varepsilon} \tag{38}$$

Then the sensitivity equation is :

$$\frac{\partial(C\tilde{T})}{\partial t} = \frac{\partial^2(k\tilde{T})}{\partial x^2} \tag{39}$$

The initial and boundary conditions are

$$\tilde{T}(x,0) = 0,\ \left.\frac{\partial(k\tilde{T})}{\partial x}\right|_{x=0} = 0,\ \left.\frac{\partial(k\tilde{T})}{\partial x}\right|_{x=L} = \left.(p'\cdot\tilde{T})\right|_{x=L} + \Delta q(t) \tag{40}$$

Adjoint Equation

Using Lagrange multiplier method and considering the initial and boundary conditions of the sensitivity problem, we get the following adjoint equation:

$$C\frac{\partial \overline{T}}{\partial t}+k\frac{\partial^2 \overline{T}}{\partial x^2}=0 \text{ or } C\frac{\partial \overline{T}}{\partial \tau}=k\frac{\partial^2 \overline{T}}{\partial x^2},\ \tau=t_f-t \tag{41}$$

$$k\frac{\partial \overline{T}}{\partial x}\bigg|_{x=0}=0,\ k\frac{\partial \overline{T}}{\partial x}\bigg|_{x=L}=(p'\cdot \overline{T})\big|_{x=L},\ \overline{T}(x,t_f)=-\frac{T(x,t_f)-T_E(x)}{C} \tag{42}$$

from which we deduce that the gradient of the error functional is

$$\nabla E=\xi q-\overline{T}(L,t) \tag{43}$$

Regular Conjugate Gradient Method

The iterative search direction may be expressed as:

$$q^{k+1}=q^k+\alpha^k P^k \tag{44}$$

$$P^k=-\nabla E^k+\beta^k P^{k-1} \tag{45}$$

The optimal step size may be derived from the value that may make the first order derivative of E in the direction α^k vanish:

$$\alpha^k=-\frac{\int_0^1 \left(T^k-T_E\right)\widetilde{T}^k dx+\xi\int_0^{t_f} q^k P^k dt}{\int_0^1 (\widetilde{T}^k)^2 dx+\xi\int_0^{t_f}(P^k)^2 dt} \tag{46}$$

The regular CG algorithm follows the procedures discussed in last section.

Modified Conjugate Gradient Method

Assume that q(t) is a continuously differentiable function

$$q(t)=\int_0^t \frac{dq(t')}{dt'}dt',\ \Delta q(t)=\int_0^t \frac{d\Delta q(t')}{dt'}dt' \tag{47}$$

which requires

$$q(t=0)=\Delta q(t=0)=0 \tag{48}$$

Similarly, we have

$$\nabla E\left(\frac{dq}{dt}\right) = \int_t^{t_f} \nabla E(q)dt' \tag{49}$$

The modified search direction is related to the derivative of the direction of decent R^k by the relation

$$p^k = \int_0^t R^k dt' \tag{50}$$

$$R^k = -\nabla E\left(\frac{dq}{dt}\right) + \gamma^k R^{k-1} \tag{51}$$

The conjugate coefficient γ^k is given by Eq. (26) and the gradient of the error function is replaced by $\nabla E\left(\frac{d\Delta q}{dt}\right)$:

$$\gamma^k = \frac{\int_0^{t_f}\left[\nabla E^k\left(\frac{dq}{dt}\right) - \nabla E^{k-1}\left(\frac{dq}{dt}\right)\right]\cdot \nabla E^k\left(\frac{dq}{dt}\right)\cdot dt}{\int_0^{t_f}\left[\nabla E^{k-1}\left(\frac{dq}{dt}\right)\right]^2 \cdot dt} \tag{52}$$

"Two-Parameter" Optimal Problem

Let us now estimate the cooling flux $q(t)$ and the heat source strength $G(t)$ simultaneously. Two constraints must be added in the system:

$$q(t) \le 0 \tag{53}$$

$$G(t) \ge 0 \tag{54}$$

This optimization problem may be classified as two-parameter constrained problem. The error functional E is now defined as:

$$E(G,q) = \frac{1}{2}\int_0^L \left[T(x,t_f) - T_E(x)\right]^2 dx + \frac{\xi_1}{2}\int_0^{t_f} G^2(t)dt + \frac{\xi_2}{2}\int_0^{t_f} q^2(t)dt \tag{55}$$

Sensitivity Equation

This problem includes two control functions, and then we must have two sensitivity temperatures:

$$\tilde{T}_1 = \lim_{\varepsilon \to 0} \frac{T(G + \varepsilon \Delta G) - T(G)}{\varepsilon} \tag{56a}$$

$$\tilde{T}_2 = \lim_{\varepsilon \to 0} \frac{T(q + \varepsilon \Delta q) - T(q)}{\varepsilon} \tag{56b}$$

which are governee bt the two following sensitivity equations

$$\begin{aligned} &\frac{\partial (C\tilde{T}_1)}{\partial t} = \frac{\partial^2 (k\tilde{T}_1)}{\partial x^2} + \Delta G \cdot H \\ &\tilde{T}_1(x,0) = 0, \left.\frac{\partial (k\tilde{T}_1)}{\partial x}\right|_{x=0} = 0, \left.\frac{\partial (k\tilde{T}_1)}{\partial x}\right|_{x=L} = \left.(p' \cdot \tilde{T}_1)\right|_{x=L} \end{aligned} \tag{57a}$$

$$\begin{aligned} &\frac{\partial (C\tilde{T}_2)}{\partial t} = \frac{\partial^2 (k\tilde{T}_2)}{\partial x^2} \\ &\tilde{T}_2(x,0) = 0, \left.\frac{\partial (k\tilde{T}_2)}{\partial x}\right|_{x=0} = 0, \left.\frac{\partial (k\tilde{T}_2)}{\partial x}\right|_{x=L} = \left.(p' \cdot \tilde{T}_2)\right|_{x=L} + \Delta q(t) \end{aligned} \tag{57b}$$

Adjoint Equation

Similarly, we have two adjoint equations:

$$\begin{aligned} &C\frac{\partial \overline{T}_1}{\partial t} + k\frac{\partial^2 \overline{T}_1}{\partial x^2} = 0 \text{ OR } C\frac{\partial \overline{T}_1}{\partial \tau} = k\frac{\partial^2 \overline{T}_1}{\partial x^2},\ \tau = t_f - t \\ &k\left.\frac{\partial \overline{T}_1}{\partial x}\right|_{x=0} = 0, k\left.\frac{\partial \overline{T}_1}{\partial x}\right|_{x=L} = \left.(p' \cdot \overline{T}_1)\right|_{x=L}, \overline{T}_1(x,t_f) = -\frac{T(x,t_f) - T_E(x)}{C} \end{aligned} \tag{58a}$$

$$\begin{aligned} &C\frac{\partial \overline{T}_2}{\partial t} + k\frac{\partial^2 \overline{T}_2}{\partial x^2} = 0 \text{ OR } C\frac{\partial \overline{T}_2}{\partial \tau} = k\frac{\partial^2 \overline{T}_2}{\partial x^2},\ \tau = t_f - t \\ &k\left.\frac{\partial \overline{T}_2}{\partial x}\right|_{x=0} = 0, k\left.\frac{\partial \overline{T}_2}{\partial x}\right|_{x=L} = \left.(p' \cdot \overline{T}_2)\right|_{x=L}, \overline{T}_2(x,t_f) = -\frac{T(x,t_f) - T_E(x)}{C} \end{aligned} \tag{58b}$$

It is found that as Eq.(58a) is exactly same as Eq (58b), the adjoint problem is to be solved only once.The gradients of the error functional in the direction of G and q are

$$\nabla E(G) = \xi_1 \cdot G - \int_0^L \overline{T}(x,t) H(x) dx \tag{59a}$$

$$\nabla E(q) = \xi_2 q - \overline{T}(L,t) \tag{59b}$$

Solution Algorithm of CGM

The iterative formula and the conjugate search direction may be expressed as:

$$G^{k+1} = G^k + \alpha_1^k P_1^k \tag{60a}$$

$$q^{k+1} = q^k + \alpha_2^k P_2^k \tag{60b}$$

$$P_1^k = -\nabla E(G)^k + \beta_1^k P_1^{k-1} \tag{61a}$$

$$P_2^k = -\nabla E(q)^k + \beta_2^k P_2^{k-1} \tag{61b}$$

$$\beta_1^k = \frac{\int_0^{t_f} (\nabla E(G)^k - \nabla E(G)^{k-1}) \nabla E(G)^k \, dt}{\int_0^{t_f} (\nabla E(G)^{k-1})^2 \, dt} \tag{62a}$$

$$\beta_2^k = \frac{\int_0^{t_f} (\nabla E(q)^k - \nabla E(q)^{k-1}) \nabla E(q)^k \, dt}{\int_0^{t_f} (\nabla E(q)^{k-1})^2 \, dt} \tag{62b}$$

The optimal step size may be derived from the values that may make the first order derivatives of E in the direction α_1^k and α_2^k equal to zero [18]. From Eq.(55), we get:

$$\begin{aligned}
\frac{\partial E}{\partial \alpha_1^k} &= \int_0^L \left[T(G^k + \alpha_1^k P_1^k, q^k + \alpha_2^k P_2^k) - T_E \right] \tilde{T}_1^k \, dx + \xi_1 \int_0^{t_f} (G^k + \alpha_1^k P_1^k) P_1^k \, dt \\
&\approx \int_0^L \left(T(G^k, q^k) - T_E + \alpha_1^k \tilde{T}_1^k + \alpha_2^k \tilde{T}_2^k \right) \tilde{T}_1^k \, dx + \xi_1 \int_0^{t_f} G^k P_1^k \, dt + \xi_1 \int_0^{t_f} \alpha_1^k (P_1^k)^2 \, dt \\
&= \int_0^L \left(T^k - T_E \right) \tilde{T}_1^k \, dx + \xi_1 \int_0^{t_f} G^k P_1^k \, dt + \alpha_1^k \left[\int_0^L (\tilde{T}_1^k)^2 \, dx + \xi_1 \int_0^{t_f} (P_1^k)^2 \, dt \right] + \alpha_2^k \int_0^L \tilde{T}_1^k \cdot \tilde{T}_2^k \, dx \\
&= 0
\end{aligned} \tag{63a}$$

and

$$\begin{aligned}
\frac{\partial E}{\partial \alpha_2^k} &= \int_0^L \left[T(G^k + \alpha_1^k P_1^k, q^k + \alpha_2^k P_2^k) - T_E \right] \tilde{T}_2^k \, dx + \xi_2 \int_0^{t_f} (q^k + \alpha_2^k P_2^k) P_2^k \, dt \\
&\approx \int_0^L \left(T(G^k, q^k) - T_E + \alpha_1^k \tilde{T}_1^k + \alpha_2^k \tilde{T}_2^k \right) \tilde{T}_2^k \, dx + \xi_2 \int_0^{t_f} q^k P_2^k \, dt + \xi_2 \int_0^{t_f} \alpha_2^k (P_2^k)^2 \, dt \\
&= \int_0^L \left(T^k - T_E \right) \tilde{T}_2^k \, dx + \xi_2 \int_0^{t_f} q^k P_2^k \, dt + \alpha_2^k \left[\int_0^L (\tilde{T}_2^k)^2 \, dx + \xi_2 \int_0^{t_f} (P_2^k)^2 \, dt \right] + \alpha_1^k \int_0^L \tilde{T}_1^k \cdot \tilde{T}_2^k \, dx \\
&= 0
\end{aligned} \tag{63b}$$

Let

$$d_1 = \int_0^L \left(T^k - T_E\right)\tilde{T}_1^k dx + \xi_1 \int_0^{t_f} G^k P_1^k dt \tag{64a}$$

$$d_2 = \int_0^L (\tilde{T}_1^k)^2 dx + \xi_1 \int_0^{t_f} (P_1^k)^2 dt \tag{64b}$$

$$d_3 = \int_0^L \left(T^k - T_E\right)\tilde{T}_2^k dx + \xi_2 \int_0^{t_f} q^k P_2^k dt \tag{64c}$$

$$d_4 = \int_0^L (\tilde{T}_2^k)^2 dx + \xi_2 \int_0^{t_f} (P_2^k)^2 dt \tag{64d}$$

$$d_5 = \int_0^L \tilde{T}_1^k \cdot \tilde{T}_2^k dx \tag{64e}$$

then Eq.(63a) and Eq.(63b) become much clear:

$$d_1 + d_2\alpha_1^k + d_5\alpha_2^k = 0 \tag{65a}$$

$$d_3 + d_4\alpha_2^k + d_5\alpha_1^k = 0 \tag{65b}$$

Solving these two linear equations, the optimal step sizes are:

$$\alpha_1^k = \frac{d_1 d_4 - d_3 d_5}{d_5^2 - d_2 d_4} \tag{66a}$$

$$\alpha_2^k = \frac{d_2 d_3 - d_1 d_5}{d_5^2 - d_2 d_4} \tag{66b}$$

The overall CGM algorithm may be summarized as follows [18,19]:

1. Set an initial initial guess $G^0 = G_0(t)$, $q^0 = q_0(t)$, set the iteration counter k = 0.

2. Solve the direct problem with G^k and q^k to obtain T^k.

3. Evaluate the difference $T^k(x, t_f) - T_E$.

4. Solve the adjoint problem backward in time for $\overline{T}_1^k$ and $\overline{T}_2^k$ ($\overline{T}_1^k = \overline{T}_2^k$).

5. Evaluate the gradients $\nabla E^k(G)$ and $\nabla E^k(q)$ according to Eq.(59).

6. Calculate the search directions P_1^k and P_2^k from Eq.(61) and Eq.(62), note that $P^k = -\nabla E^k$ if k=0.

7. Solve the sensitivity problems with $\Delta G = P_1^k$, $\Delta q = P_2^k$ to obtain $\tilde{T}_1^k$ and $\tilde{T}_2^k$.

8. Calculate the step sizes α_1^k and α_2^k with Eq. (66).

9. Update to $G^{k+1} = G^k + \alpha_1^k P_1^k$, $q^{k+1} = q^k + \alpha_2^k P_2^k$.

10. Set k = k + 1, go back to step 2, repeat until convergence criterion $E^k < \varepsilon$ is satisfied.

Results and Discussion

In this study, we choose A356 Aluminum to test our solution algorithm. The thermo-physical and electromagnetic properties of this light metal alloy are shown in Table 1 [7, 22], the other parameters used in the calculations are presented in Table 2. The resistivity of the material should be proportional to the temperature and the surface emissivity of metal is variable with temperature and oxidation during the heating. However, these two parameters are assumed to be constants in this report since this hypothesis would not influence the final results too much.

Table1: Thermo-physical and electromagnetic properties of A356

Density (kg/m^3)	-0.208 T($^\circ C$)+2680.0
Specific heat ($J/kg\cdot^\circ C$)	0.454 T($^\circ C$)+904.6
Thermal Conductivity ($W/m\cdot^\circ C$)	0.04 T($^\circ C$)+153.1
Solidus temperature ($^\circ C$)	550
Liquid temperature ($^\circ C$)	615
Heat convection coefficient ($W/m^2\cdot^\circ C$)	5
Resistivity ($\Omega\cdot m$)	8.0 x10^{-8}
Relative magnetic permeability	1.0

Table 2: Parameters in calculations

Current frequency (Hz)	10000
Ambient Temperature ($^\circ C$)	20

Targeted Temperature (°C)	530
Emissivity (Aluminum Alloy)	0.1
Emissivity (Ceramic Pedestal)	0.94
Maximum Input Power (W)	8000
Electrical Efficiency of Induction Heater (%)	79.4

Optimal Heating Strategy

In this section, the forced convection cooling flux is supposed to be known. From Eq.(5), the input power may be expressed as:

$$P(t)=\frac{1}{\eta_E}\iiint_V S(x,t)dV=G(t)\iiint_V e^{-2(L-x)/\delta}dV \tag{67}$$

It follows that

$$\frac{P(t)}{P_{max}}=\frac{G(t)}{G_{max}} \tag{68}$$

Our purpose is to heat the material up to 530℃ and require the final temperature distribution as uniform as possible. If the objective function G(t) is determined, then the optimal heating strategy , namely P(t) is obtained. We must note that G(t) should be equal to or be greater than zero. This constrained condition must be added into the optimization problem which then becomes a constrained minimization problem. In this study, the maximum power is known as 8KW and the efficiency of induction unit is supposed to be 79.4%.

One Stage Heating

Let us consider the possibility of one stage heating which is the simplest method. Firstly, we choose a medium power level $P(t)=0.61P_{max}$ and an operating frequency of 10KHz. Because the material is heated with a constant internal heat source, the temperature within the work-piece increases almost linearly (FIG.3.1). After 240 seconds, the surface temperature is about 542.5℃ while the central temperature just reaches 520℃. FIG.3.2 shows a typical surface-to-core temperature profile. Such a big temperature difference cannot be accepted.

According to the knowledge of heat transfer and electronics, there are four possible ways to reduce the temperature difference:

1) Decrease the frequency of the induction unit;

2) Decrease the radius of the work-piece;

3) Cooling the surface of the work-piece;

4) Extend the heating process.

From Eq.(4) and Eq.(6), we know that methods (1) and (2) may effectively improve the uniformity of heat source distribution. If the operating frequency is reduced to 500Hz and all other conditions remain the same, the maximum temperature difference at the final time is less than 20℃; comparing with the frequency of 10KHz, T_{suface}-T_{center} decreases 2.5℃ (FIG.4). However, this result is still not good enough, and lower frequencis are not permitted in commercial induction machines.

Now let us use method (3) by cooling the surface with a constant flux of$1.0\times10^5\,\mathrm{W/m^2}$. In order to compensate for this heat loss, the input power has to be increased to 0.89P_{max}. From FIG.5, it is found that the temperature difference at the end of heating process is almost same as that obtained without cooling. In fact, for A356 and a frequency of 10KHz, the skin depth is only 1.42mm, i.e.the compensatory heat is concentrated in the surface region. Then the surface temperature almost doesn't change. So cooling the surface with a constant flux is not an effective approach to eliminate the temperature difference for this kind of metal alloy heated by a relatively high frequency.

The effect of total heating time is also examined. The heating time is longer, the required input power is lower and vice versa. The essential mechanism of heat conduction is the heat diffusion from high temperature region to lower temperature region. It is known that the longer heating time as well as diffusion time allows more heat to be transferred from surface region to center region and therefore reduces the temperature gradient (the input heat is fixed). Two cases of final times, t_f=200s and t_f=300s, are tested respectively, the induction frequency is 10KHz. For the former case, the maximum temperature difference is about 26.5℃; and for the latter case, it decreases to

18℃. The corresponding results are shown in FIG.6 and FIG.7. It appears that a much longer heating time may be necessary to significantly improve the uniformity of the final temperature distribution. When the final time is prolonged to 600 seconds, the temperature difference is about 9℃ (FIG.8) which is within an acceptable range.

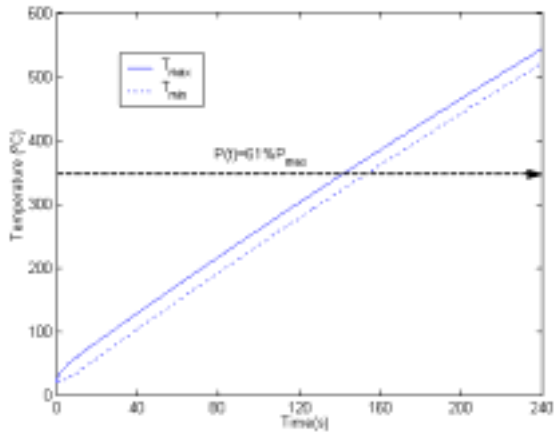

FIG.3.1: Temperature Evolution
q(t)=0, f=10000Hz, t_f=240s

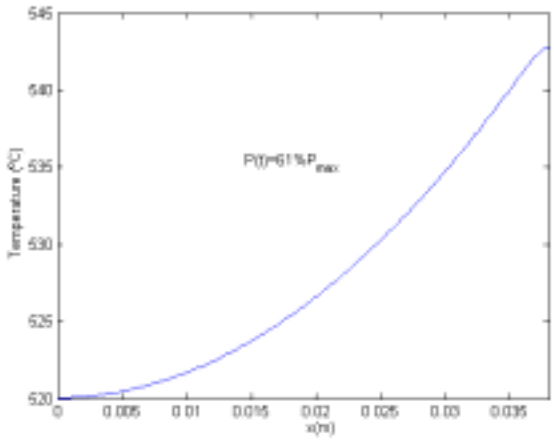

FIG.3.2: Surface-to-Core Profile
q(t)=0, f=10000Hz, t_f=240s

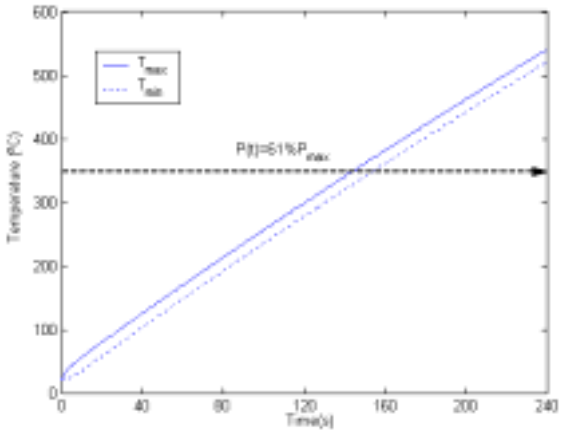

FIG.4.1: Temperature Evolution
q(t)=0, f=500Hz, t_f=240s

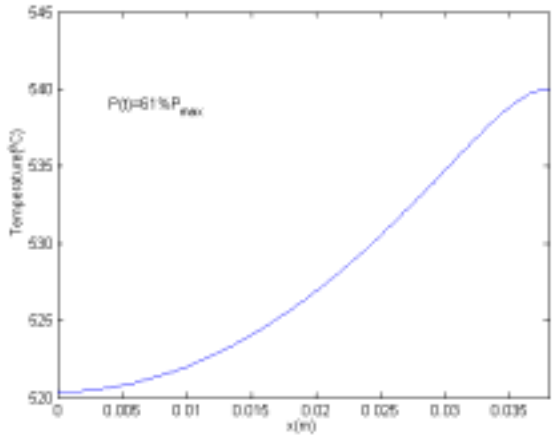

FIG.4.2: Surface-to-Core Profile
q(t)=0, f=500Hz, t_f=240s

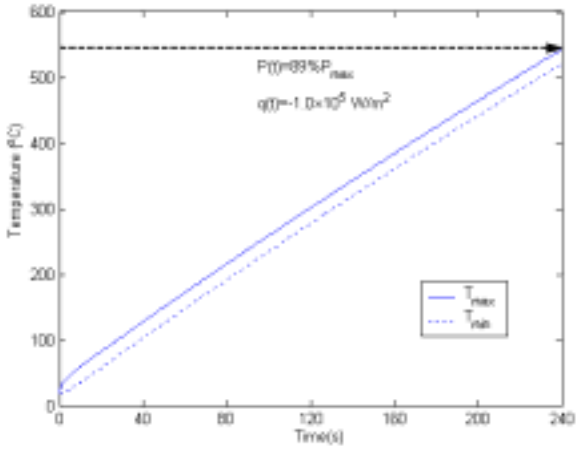

FIG.5.1: Temperature Evolution
q(t)=-1.0E5 W/m^2, f=10000Hz, t_f=240s

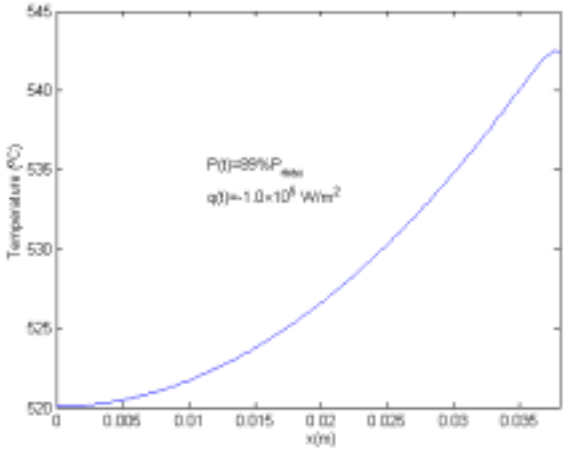

FIG.5.2: Surface-to-Core Profile
q(t)=-1.0E5W/m^2, f=10000Hz, t_f=240s

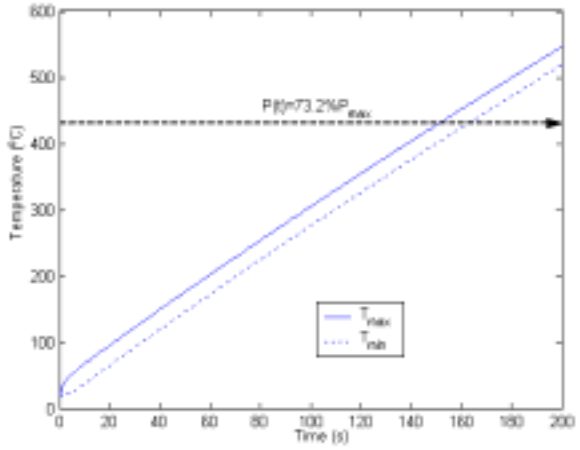

FIG.6.1: Temperature Evolution
q(t)=0, f=10000Hz, t_f=200s

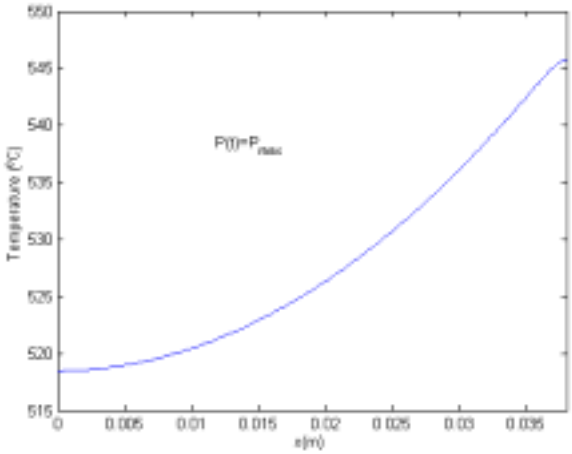

FIG.6.2: Surface-to-Core Profile
q(t)=0, f=10000Hz, t_f=200s

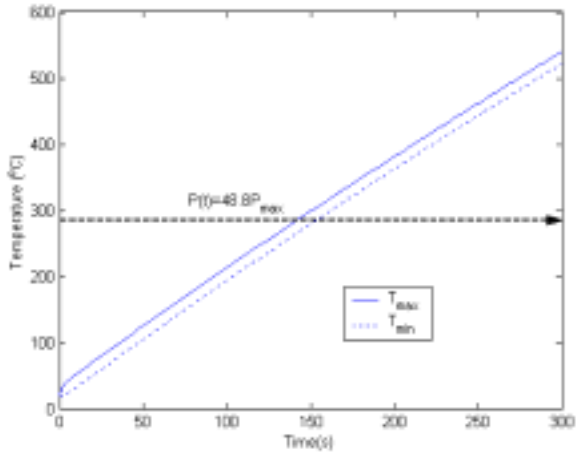

FIG.7.1: Temperature Evolution
q(t)=0, f=10000Hz, t_f=300s

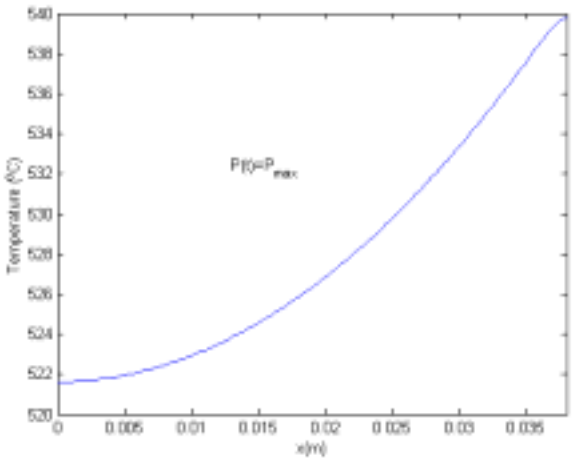

FIG.7.2: Surface-to-Core Profile
q(t)=0, f=10000Hz, t_f=300s

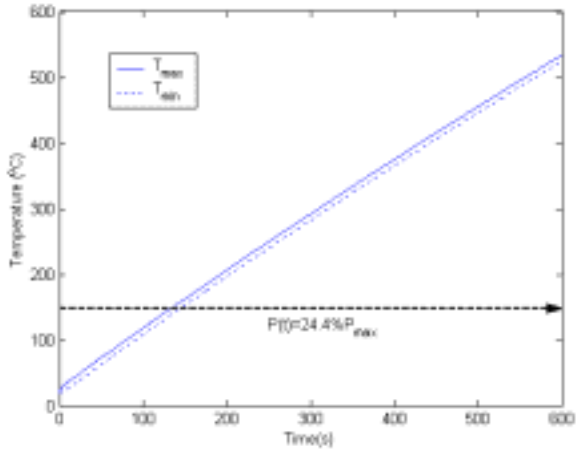

FIG.8.1: Temperature Evolution
q(t)=0, f=10000Hz, t_f=600s

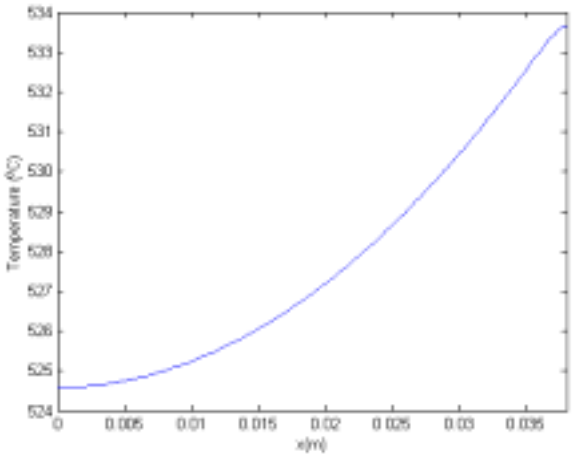

FIG.8.2: Surface-to-Core Profile
q(t)=0, f=10000Hz, t_f=600s

Based on the above results, we may conclude that changing the induction frequency and cooling the material surface do not decrease significantly the thermal gradient at the final time. Extending the heating process may be an effective approach. However, the minimum time of 10 minutes would not satisfy the productivity requirements. On the other hand, the technology of thixoforming also requires a short reheating process to maintain the initial microstructure. So a one-stage heating is not adapted to the semi-solid forming for an A356 billet with a 76mm diameter.

Optimal Solution by CGM

In order to achieve a uniform temperature distribution in the work-pieces in the shortest possible heating time, researchers working in the domain of semi-solid forming normally adopted a multi-step heating strategy. Such optimal procedures were determined empirically [3]. Bendada et al. [29] proposed two two-stage heating methods: 1) start heating at a high-power level for 205s, then switch to a low-power stage during 35s; 2) start heating at a high-power level for 140s, then switch to a low-power stage for 100s. We apply these two procedures to our model and solve the direct problem (FIG.9.1), the surface-to-core temperature profile with a maximum temperature difference of about 2.5℃ at the end of

heating is obtained (FIG.9.2). However, there exists overheating which occurs around the switching times 205s and 140s (FIG.9.3) and the maximum surface temperature exceeds the targeted value about 11℃. If the overheating of 11℃ takes place in semi-solid state, the liquid fraction in surface region would go up to 70%. It may lead to the so-called 'elephant foot' effect. The authors of [29] clearly observed this phenomenon when the strategy B is performed. The relatively straight wall was produced while executing strategy A. They also concluded that the switching time has a major impact on the development of an 'elephant foot' as the overheating cannot be avoided.

Now let us look at the optimal solutions obtained by regular CGM. In order to compare with the experimental solutionsA and B, a final time of 240s is firstly tested. After 61 iterations which start from an initial guess of zero, we obtain a similar solution as strategy A (FIG.9.1), and the maximum temperature difference is less than 1.5℃ (FIG.9.2). However, the surface overheating phenomenon still exits, at t=233s, T_{max} reaches 540℃ (see FIG.9.3). On the other hand, this optimal solution requires the input power changes steeply from high-power level to zero within 17 seconds. It would be very hard to execute such a curve exactly. Then we make a two-stage strategy based on the approximation of this continuous optimal heating curve: heating the work-piece with 64% of maximum power capacity until t=230s, then turning off the induction heater and holding for 10 seconds. From FIG.10, it is found that the temperature distribution becomes more uniform, T_{max}-T_{min} is only 0.6℃. However, the surface overheating is more serious, the surface temperature at t=230s reaches 545.7℃. Although the switching time is close to the final time, 'elephant foot' phenomenon is possible to take place. So an experiment is necessary to test this heating control strategy, and some modification may be needed.

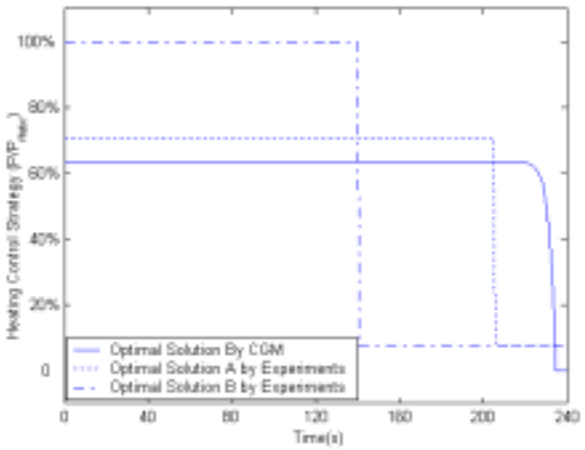

FIG.9.1: Optimal Heating Strategy
q(t)=0, f=10000Hz, t_f=240s

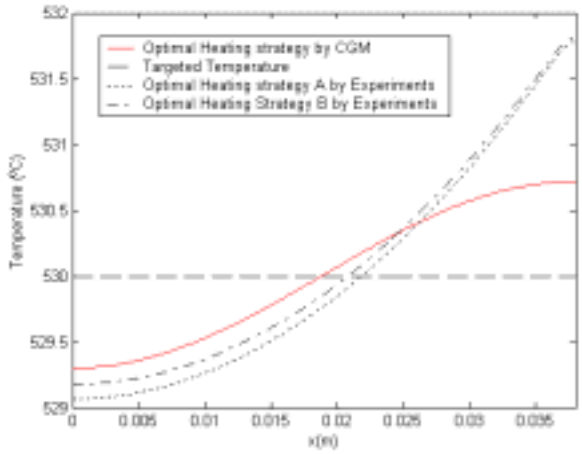

FIG.9.2: Temperature distribution at final time
q(t)=0, f=10000Hz, t_f=240s

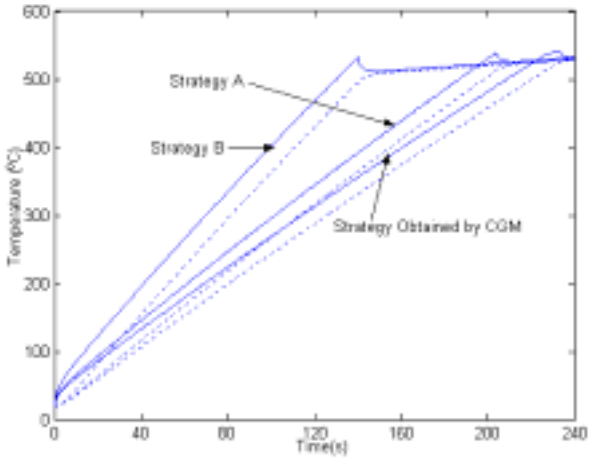

FIG.9.3: Evolution of Surface and Central Temperature
f=10000Hz

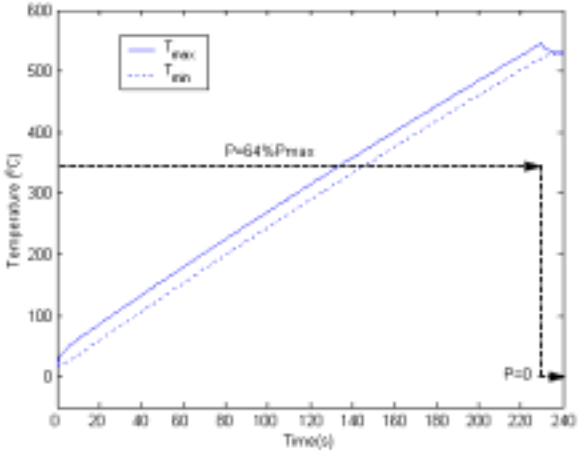

FIG.10.1: Approximative Heating Strategy

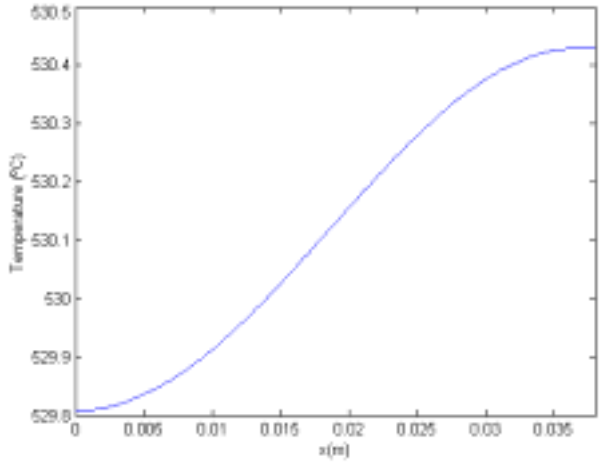

FIG.10.2: Temperature distribution at final time

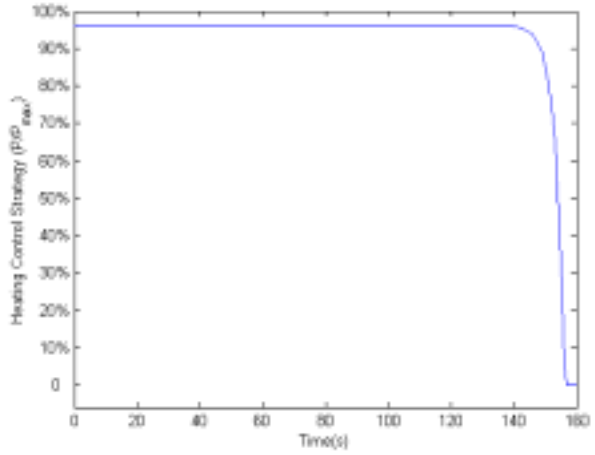

FIG.11.1: Optimal Heating Strategy
q(t)=0, f=10000Hz, t_f=160s

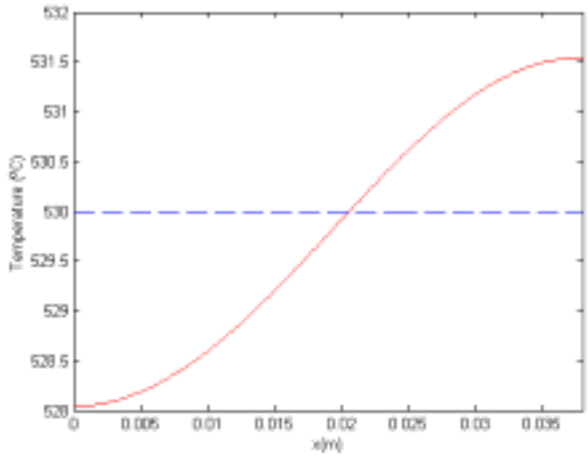

FIG.11.2: Temperature distribution at final time
q(t)=0, f=10000Hz, t_f=160s

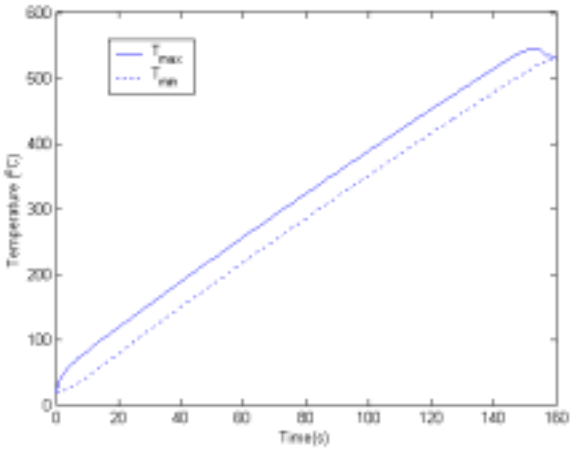

FIG.11.3: Evolution of Surface and Central Temperature
f=10000Hz

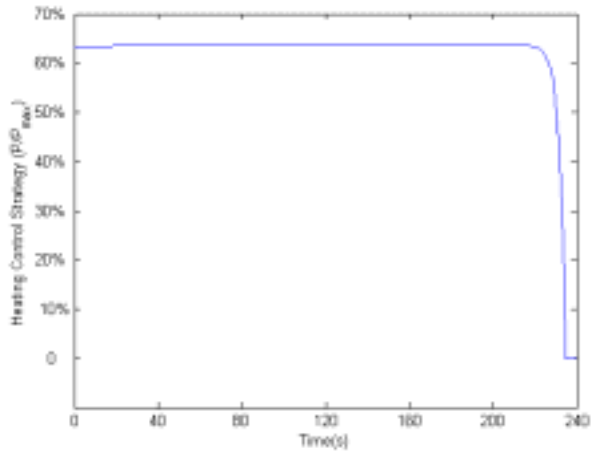

FIG.12.1: Optimal Heating Strategy
q(t)=0, f=500Hz, t_f=240s

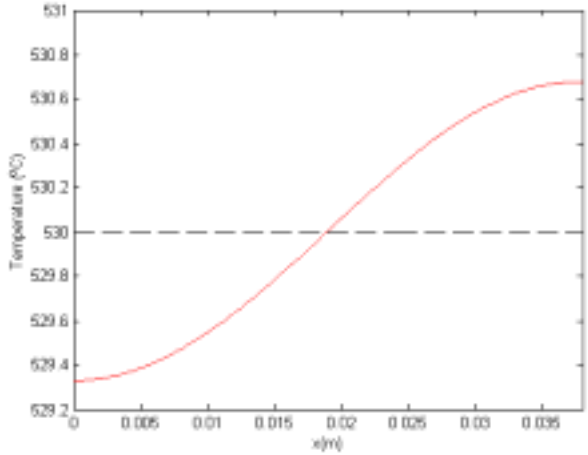

FIG.12.2: Temperature distribution at final time
q(t)=0, f=500Hz, t_f=240s

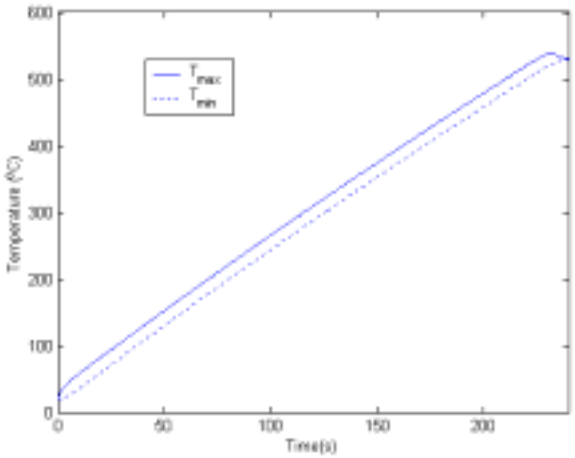

FIG.12.3: Evolution of Surface and Central Temperature
f=500Hz

If the total heating time is reduced to 160 second, satisfactory temperature uniformity can still be obtained (FIG.11). However, the maximum surface temperature increases 5℃. To avoide the 'elephant foot', we don't suggest shortening the heating process further.

At last, we also examine case of low frequency. As expected, a frequency of 500Hz almost does not affect the final temperature distribution. According to the discussion above, we may conclude that an optimal heating control strategy which leads to a uniform final temperature distribution may be obtained by using conjugate gradient method. The approximative solution by dividing the continuous optimal heating curve to two stages facilitates the operating of induction heater. However, there exists a risk of 'elephant foot' because of the overheating in surface region cannot be avoided.

Optimal Solution by Modified CGM

As we have discussed in previous section, the optimal heating profile obtained by regular CGM is difficult to realize because of the sharp descent near the final time. Recently Jiang, Nguyen and Prud'homme [24] found that a modified CGM is more powerful than regular CGM to solve this kind of inverse heat transfer problem. In this study, we follow this

modification to resolve the optimal control problem. Since the current frequency and surface cooling will not improve the temperature uniformity, the cooling flux is set to zero and the frequency is fixed as 10KHz. Because the optimal solution at t=0 always equals to initial guess value, then the initial guess is very important to the solution profile. When initial Guess G^0/G_{max} is set 100%, a smooth heating control curve which requires reducing the input power gradually from maximum to zero is estimated by using the modified CGM (see FIG.13.1). The final temperature uniformity is perfectly achieved after 5 iterations: T_{max}-T_{min} is only 0.25℃ (FIG.13.2). Furthermore, the surface temperature also increases smoothly, there is no surface overheating because the maximum surface temperature is less than 531℃ (FIG.13.3). In other words, 'elephant foot' phenomenon will not occur. If the initial Guess G^0/G_{max} is set to 80%, except that the heating curve is affected, all the control parameters include convergence rate change little (FIG.14). When the final time is reduced to 120 seconds, the surface overheating is not considerable, the temperature uniformity at the final time remains perfect. But the maximum input power should increase to a double value. Shorter heating procedure may result in a more serious surface heating, so it is not suggested.

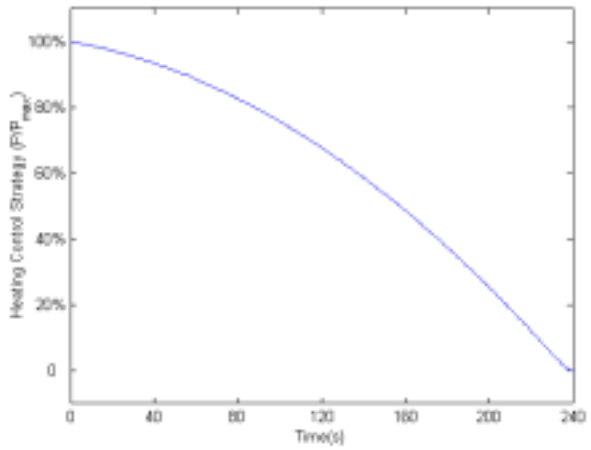

FIG.13.1: Optimal Heating Strategy
Initial Guess G^0/G_{max}= 100%

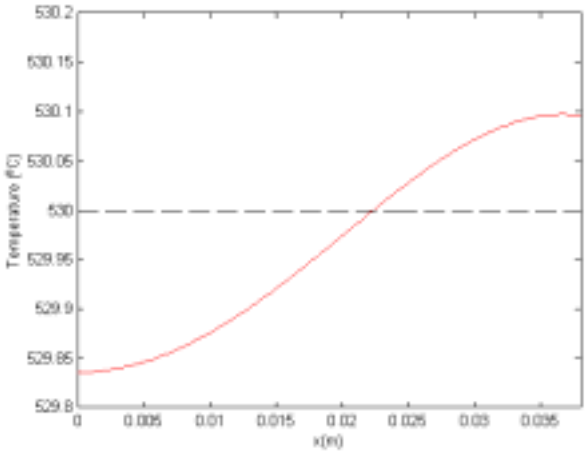

FIG.13.2: Temperature distribution at final time
q(t)=0, f=10000Hz, t_f=240s

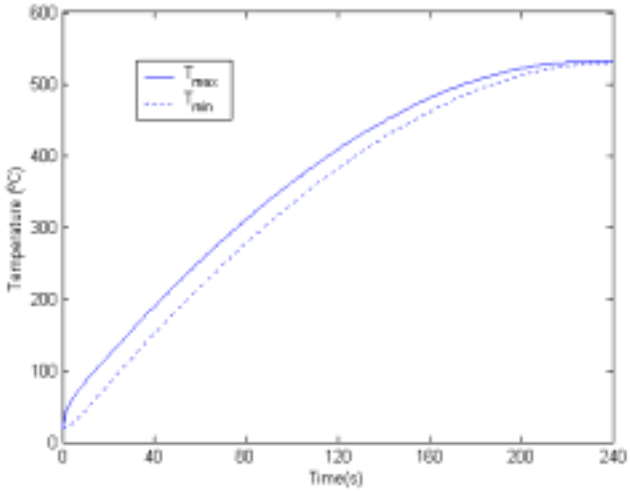

FIG.13.3: Evolution of Surface and Central Temperature

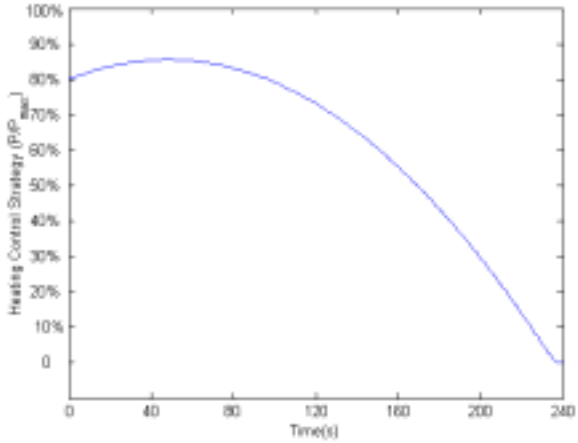

FIG.14.1: Optimal Heating Strategy
Initial Guess G^0/G_{max}= 80%

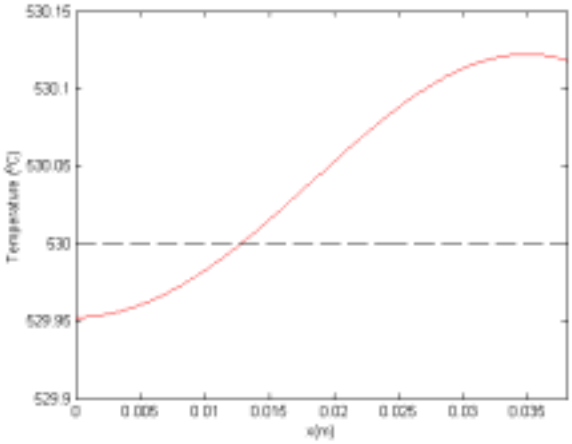

FIG.14.2: Temperature distribution at final time
q(t)=0, f=10000Hz, t_f=240s

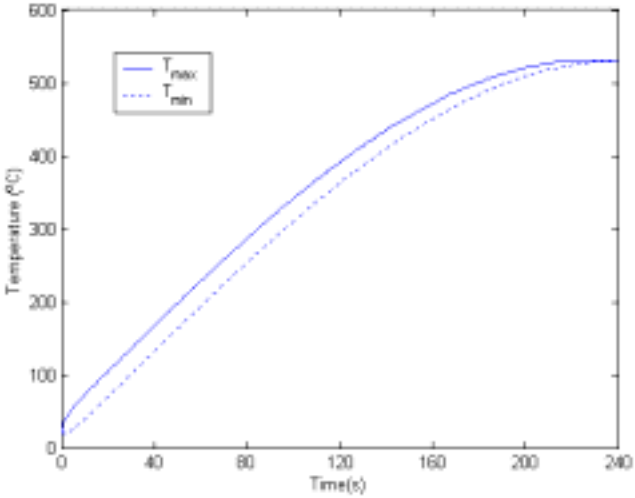

FIG.14.3: Evolution of Surface and Central Temperature

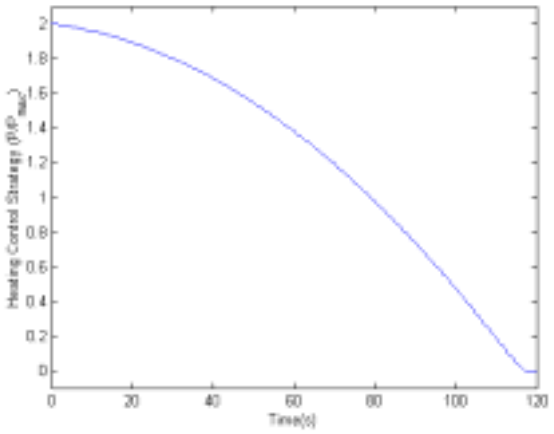

FIG.15.1: Optimal Heating Strategy
Initial Guess G^0/G_{max}= 200%

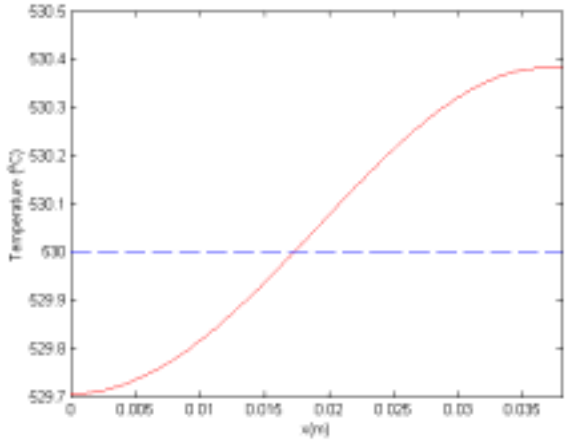

FIG.15.2: Temperature distribution at final time
q(t)=0, f=10000Hz, t_f=120s

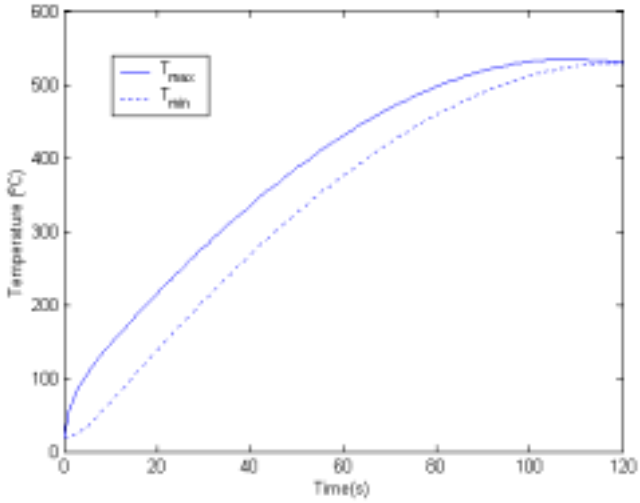

FIG.15.3: Evolution of Surface and Central Temperature

On Optimal Cooling

In this section, a one-stage heating procedure is fixed; an optimal cooling strategy obtained by CGM may considerably eliminate the temperature difference at the final heating time. However, the surface overheating cannot be controlled effectively. The corresponding results are shown in FIG.16. In addition, such a cooling process must be performed precisely in the last 10 seconds. It will be very hard to be realized in real situations. Since the cooling flux q(t) must be less than or equal to zero, this problem is also a constrained optimization problem. Modified CGM is found to fail because the constraint results in the divergence of the solution.

On the other hand, the surface cooling may lead to the additional energy loss which decreases the efficiency of the heat processing. Although the theoretical solution can be obtained, we do not suggest applying this optimal cooling approach.

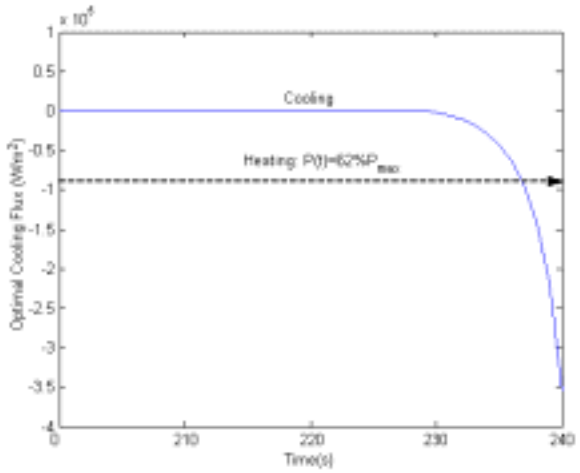

FIG.16.1: Optimal Cooling Strategy
f=10000Hz, t_f=240s

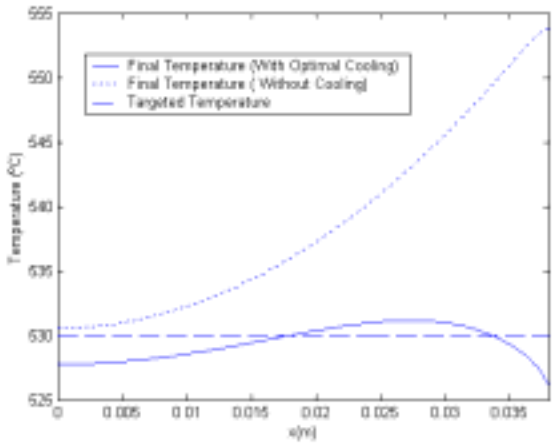

FIG.16.2: Temperature distribution at final time
f=10000Hz, t_f=240s

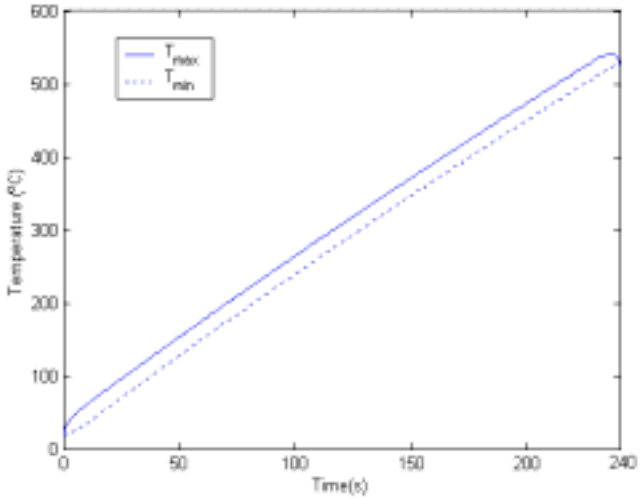

FIG.16.3: Evolution of Surface and Central Temperature

Conclusion

This study examines the various possible approaches to achieve the uniform temperature distribution at the end of the heat processing. It is found that changing the current frequency of induction unit or cooling the

material surface with a constant flux cannot improve the temperature uniformity effectively. Optimal cooling method is also not suggested since the cooling strategy obtained by CGM is not practicable. The optimal heating strategy obtained by regular CGM may eliminate the temperature difference, but the surface overheating cannot be avoided. And the sharp descent heating curve has to be modified to be practicable. Modified CGM is probably the best approach to solve this optimal control problem because its solution obtained after 5 iterations may eliminate both the temperature gradient at the final time and the surface overheating. And the heating process may be reduced to 120 seconds.

References

[1] S. Midson, K.Brissing, *Semi-Solid Casting of Aluminum Alloys*: *A Status Report*, Modern Casting, pp.41-43, 1997.

[2] S. Midson, V. Rudnev and R. Gallik, *Semi-Solid Processing of Aluminum Alloys*, Industrial Heating, pp.37-41, 1999.

[3] H.K. Jung, C.G. Kang, *Induction Heating Process of an Al-Si Aluminum Alloy for Semi-Solid Die Casting and Its Resulting Microstructure*, Journal of Materials Processing Technology, Vol.120, pp.355-364, 2002.

[4] Y. Ono, C.Q. Zheng, F.G. Hamel, R. Charron and C.A. Loong, *Experimental Investigation on Monitoring and Control of Induction Heating Process for Semi-Solid Alloys Using the Heating Coil as Sensor*, Measurement Science and Technology, Vol.13, pp1359-1365, 2002.

[5] D-C Ko, G-S Min, B-M, Kim, J-C, Choi, *Finite Element Analysis for the Semi-Solid State Forming of Aluminum Alloy Considering Induction Heating*, Journal of Materials Processing Technology, Vol.100, pp.95-104, 2000.

[6] M.C. Flemings, *Behavior of Metal Alloys in the Semi-solid State*, Met. Trans. A22, pp.957-981, 1991.

[7] K.T. Nguyen and A. Bendada, *An Inverse Approach for the Prediction of the Temperature Evolution During Induction Heating of a Semi-Solid Casting Billet*, Modelling Simul. Mater. Sci. Eng. Vol.8, pp.857-870, 2000.

[8] S. Midson, V. Rudnev and R. Gallik, *The Induction Heating of Semi-Solid Aluminum Alloys*, Proc. 5th Int. Conf. on Semi-Solid Processing of Alloys and Composites (Golden, CO), pp.497-504, 1998.

[9] A. Bendada, K.T. Nguyen and C.A. Loong, *Application of Infrared Imaging in Optimizing the Induction Heating of Semi-Solid Aluminum Alloys*,

Proc. Int, Symp. On Advanced Sensors for Metals Processing (Quebec), pp331-342, 1999.
[10] P. Kapranos, R.C. Gibson, D.H. Kirkwood and C.M Sellars, *Induction Heating and Partial Melting of High Melting Point Thixoformable Alloys*, Proc. 4th Int. Conf. on Semi-Solid Processing of Alloys and Composites (Sheffield), pp148-152, 1996.
[11] A.G. Butkovskii and A.Y. Lerner, *The Optimal Control Systems with Distributed Parameter*, Auto. Remote Control, Vol.21, pp.472-477, 1960.
[12] Y. Sakawa, *Solution of an Optimal Control Problem in a Distributed-Parameter System*, IEEE Trans. Auto. Contr. Vol. AC-9, No.4, pp.420-426, 1964.
[13] Y. Sakawa, *Optimal Control of a Certain Type of Linear Distributed-Parameter System*, IEEE Trans. Auto. Contr. Vol. AC-11, No.1, pp.35-41, 1966.
[14] R.K. Cavin and S.C. Tandon, *Distributed Parameter System Optimum Control Design via Finite Element Discretization,* Automatica, Vol.13, pp.611-614, 1977.
[15] R.A. Meric, *Finite Element Analysis of Optimal Heating of a Slab with Temperature Dependent Thermal Conductivity*, Int, Journal Heat and Mass Transfer, Vol.22, pp.1347-1353, 1979.
[16] R.A. Meric, *Finite Element and Conjugate Gradient Methods for a Nonlinear Optimal Heat Transfer Control Problem*, Int, J. Numer. Meth. Eng., Vol.14, pp.1851-1863, 1979.
[17] C.T. Kelley and E. W. Sachs, A *Trust Region Method for Parabolic Boundary Control Problems*, SIAM J. Optimization., Vol.9, No.4, pp. 1064-1081, 1999.
[18] C.H. Huang, *A Nonlinear Optimal Control Problem in Determining the Strength of the Optimal Boundary Heat Fluxes*, Numerical Heat Transfer, Part B, Vol.40, pp.411-429, 2001.
[19] C.H. Huang and C.Y. Li, *A Three-Dimensional Optimal Control Problem in Determining the Boundary Control Heat Fluxes*, Heat and Mass Transfer, Vol.39, pp. 589-598, 2003.
[20] C.J. Chen and M.N. Ozisik, *Optimal Heating of a Slab with a Plane Heat Source of Timewise Varying Strength*, Numerical Heat Transfer, Part A, Vol. 21, pp.351-361, 1992.
[21] C.J. Chen and M.N. Ozisik, *Optimal Heating of a Slab with Two Plan Heat Sources of Timewise Varying Strength*, J. Franklin Inst., Vol. 329, pp.195-206, 1992.
[22] M. Orfeuil, Electric Process Heating: Technologies/Equipment /Applications, Battelle Press, 1981.
[23] H. Jiang, T. H. Nguyen and M. Prud´homme, *Control of the Boundary Heat Flux during the Heating Process of a Solid Material*, International Communications in Heat and Mass Transfer, Vol.32, No.6, pp.728-738, 2005.

[24] H. Jiang, T. H. Nguyen and M. Prud´homme,*Inverse Unsteady Heat Conduction Problem of Second Kind*, Technical Report, Ecole Polytechnique de Montréal, EPM-RT-2005-06.
[25] C.H. Huang and M.N. Özisik, *Inverse Problem of Determining Unknown Wall Heat Flux in Laminar Flow Through a Parallel Plate Duct*, Numerical Heat Transfer, Part A, 21, pp.55-70 ,1992.
[26] H. M. Park and O. Y. Chung, *An Inverse Natural Convection Problem of Estimating the Strength of a Heat Source*, Int. J. Heat Mass Transfer, 42, pp. 4259-4273, 1999.
[27] H.M. Park and W.S. Jung, *The Karhunen-Loève Galerkin Method for the Inverse Natural Convection Problems*, Int. J. Heat Mass Transfer, 44, pp. 155-167 , 2001.
[28] S. Jasmin and M. Prud´homme, *Inverse determination of a heat source from a solute concentration generation model in porous medium*, Int. J. Heat Mass Transfer, 2004.
[29] A. Bendada, C.Q. Zheng and N. Nardini, *Investigation of Temperature Control Parameters for Inductive Heated Semi-Solid Light Alloys Using Infrared Imaging and Inverse Heat Conduction,* Journal of Physics D: Applied Physics, Vol. 37, pp.1137-1144, 2004.

L'École Polytechnique se spécialise dans la formation d'ingénieurs et la recherche en ingénierie depuis 1873

École Polytechnique de Montréal

École affiliée à l'Université de Montréal

Campus de l'Université de Montréal
C.P. 6079, succ. Centre-ville
Montréal (Québec)
Canada H3C 3A7

www.polymtl.ca

ÉCOLE
POLYTECHNIQUE
MONTRÉAL